Conditions for repulsive Casimir forces between identical birefringent materials

David A. T. Somers and Jeremy N. Munday

Phys. Rev. A **95**, 022509 — Published 23 February 2017

DOI: 10.1103/PhysRevA.95.022509

Conditions for repulsive Casimir forces between identical birefringent materials

David A.T. Somers[1,2] and Jeremy N. Munday[2,3]

[1] *Department of Physics, University of Maryland, College Park, MD 20740, USA*
[2] *Institute for Research in Electronics and Applied Physics, University of Maryland, College Park, MD 20740, USA*
[3] *Department of Electrical and Computer Engineering, University of Maryland, College Park, MD 20740, USA*

(Dated: January 10, 2017)

Repulsive Casimir-Lifshitz forces are known to exist between two dissimilar materials if a third material, whose dielectric response is intermediate, separates them. However, the force between two identical materials is almost always attractive. Here we show that the force between two identical, semi-infinite birefringent slabs can be repulsive for particular orientations and compare the conditions for repulsion in this system to those of isotropic materials. We examine the dependence of the Casimir-Lifshitz force on retardation and relative orientation in this system and discuss situations in which the force can be changed from attractive to repulsive as a function of both distance and rotation angle.

I. INTRODUCTION

Since its original derivation in 1948 [1], the Casimir effect has been the subject of many experimental and theoretical investigations. The original paper predicted an attractive force between perfect conductors separated by vacuum, but the result has been generalized to include more complicated materials and geometries [2–5]. In particular, Barash calculated the force and torque experienced by two semi-infinite anisotropic materials separated by a dielectric medium [4]. There have been many experiments that confirm predictions from Lifshitz's theory [6–11], and several experiments have been proposed to measure the torque between anisotropic materials [12–16].

Because attractive Casimir-Lifshitz forces can cause stiction in MEMS or NEMS devices [17], there has been significant effort to engineer systems that exhibit Casimir-Lifshitz repulsion. So far, repulsion has only been measured between two dissimilar materials separated by a third material which has a dielectric response intermediate to the other materials [7, 18]. Some theoretical works have proposed other systems that could exhibit Casimir repulsion. The most common approach among these includes metamaterials with strong magnetic responses at optical frequencies, such as in [19–21]. Rosa *et al.* considered uniaxial out-of-plane metamaterials (among other anisotropic materials), but focused on planar systems separated by vacuum [22]. These systems all require at least one of the plates to have a strong magnetic response. There have also been numerical and analytical studies of geometries that could produce repulsion between metals separated by vacuum, but these systems are unstable to lateral perturbations and therefore difficult to realize experimentally [23, 24]. Deng *et al.* predicted an attractive-repulsive transition of the force between an aligned, uniaxial, in-plane material and a conducting surface separated by vacuum as a function of distance [25]. This system also relies on the magnetic response of the plates to produce repulsion.

However, there is another less commonly discussed system that exhibits Casimir repulsion: nonmagnetic dielectrics with uniaxial in-plane birefringence separated by a dielectric medium, as first noted in [5]. For this case, two *identical* materials can exhibit Casimir-Lifshitz repulsion under specific orientations. Although two planar dielectric bodies with reflective symmetry are always attracted [26], a rotational displacement between the two anisotropic materials breaks the reflective symmetry of the system. The force is always attractive when the axes of symmetry are aligned, but can become repulsive when the symmetry is broken. Here we expand on [5] to outline the conditions for which Casimir-Lifshitz repulsion may occur for two identical, anisotropic materials.

II. NONRETARDED HAMAKER COEFFICIENTS FOR ANISOTROPIC SYSTEMS

We consider two identical, semi-infinite slabs of uniaxial birefringent materials with optical axes in the x-y plane, but rotated with respect to each other (Fig. 1b). Their permittivity tensors are:

$$\boldsymbol{\varepsilon_1} = \begin{pmatrix} \varepsilon_\parallel & 0 & 0 \\ 0 & \varepsilon_\perp & 0 \\ 0 & 0 & \varepsilon_\perp \end{pmatrix}, \tag{1a}$$

$$\boldsymbol{\varepsilon_2} = \begin{pmatrix} \varepsilon_\parallel \cos^2\theta + \varepsilon_\perp \sin^2\theta & (\varepsilon_\perp - \varepsilon_\parallel)\sin\theta\cos\theta & 0 \\ (\varepsilon_\perp - \varepsilon_\parallel)\sin\theta\cos\theta & \varepsilon_\parallel \sin^2\theta + \varepsilon_\perp \cos^2\theta & 0 \\ 0 & 0 & \varepsilon_\perp \end{pmatrix}, \tag{1b}$$

where θ is the relative angle between the optical axes of the materials. When their axes are aligned, $\theta = 0$ and $\boldsymbol{\varepsilon_1} = \boldsymbol{\varepsilon_2}$. The Helmholtz free energy per unit area of this system at finite temperature was derived by Barash [4]:

$$\Omega(d,\theta) = \frac{k_\mathrm{B}T}{4\pi^2} {\sum_{n=0}^{\infty}}' \int_0^\infty r\mathrm{d}r \int_0^{2\pi} \mathrm{d}\varphi \ln D_n(d,\theta,r,\varphi), \tag{2}$$

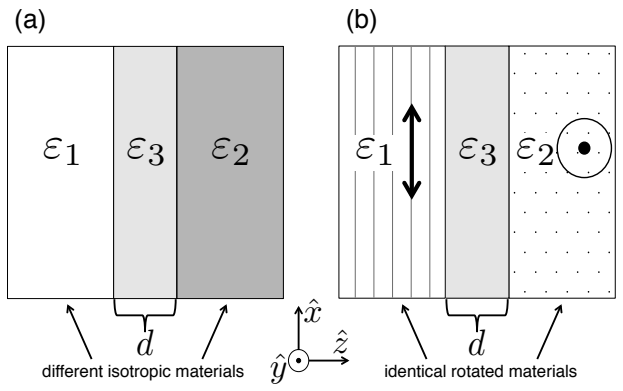

FIG. 1. Schematic of the systems under investigation. Two infinite dielectric slabs interact across a third dielectric of width d. We compare the Casimir-Lifshitz interaction in (a) the case of two isotropic slabs with dielectric functions ε_1 and ε_2 to (b) the case with two identical birefrigent materials with dielectric function $\varepsilon_\parallel$ along the principal axis and $\varepsilon_\perp$ in the other directions. In (b) the optical axis for material one is along the x-axis while that of material two is rotated by $\theta = \pi/2$.

where the summand is evaluated at the imaginary Matsubara frequencies $\mathrm{i}\xi_n = \mathrm{i}n2\pi k_\mathrm{B}T/\hbar$, the prime indicates that the $n = 0$ term is to be halved, and variables r and φ are radial and azimuthal components of the wave-vector. The full form of D_n is derived in [4] and reproduced in [14, 27]. In the nonretarded limit (corresponding to the van der Waals regime), the Casimir-Lifshitz free energy is expressed in terms of a Hamaker coefficient, which is independent of d:

$$\Omega(d,\theta) = -\frac{A_\mathrm{Ham}}{12\pi d^2} \tag{3}$$

resulting in a force given by

$$F(d,\theta) = -\frac{\partial\Omega(d,\theta)}{\partial d} = -\frac{A_\mathrm{Ham}}{6\pi d^3}. \tag{4}$$

The sign of the Hamaker coefficient gives the sign of the force, with $A_\mathrm{Ham} > 0$ indicating attraction and $A_\mathrm{Ham} < 0$ indicating repulsion.

The dispersion condition can be written as a function of the Fresnel reflection matrices of the two interfaces, as in [22, 28]:

$$D_n = \det\left(\mathbf{I} - \mathbf{r}_1\mathbf{r}_2 e^{2\rho_m d}\right) \tag{5a}$$

$$\mathbf{r}_i = \begin{pmatrix} r_i^{ss} & r_i^{sp} \\ r_i^{ps} & r_i^{pp} \end{pmatrix}. \tag{5b}$$

In the nonretarded approximation, $r_i^{ss} = r_i^{sp} = r_i^{ps} = 0$, and only r_i^{pp} (corresponding to TM modes) remains, so that:

$$D_n = 1 - r_1^{pp} r_2^{pp} e^{-2\rho_3 d}, \tag{6a}$$

$$r_i^{pp} = \frac{\varepsilon_3 - \varepsilon_\perp\sqrt{1 + \left(\varepsilon_\parallel/\varepsilon_\perp - 1\right)\cos^2\left(\theta_i + \varphi\right)}}{\varepsilon_3 + \varepsilon_\perp\sqrt{1 + \left(\varepsilon_\parallel/\varepsilon_\perp - 1\right)\cos^2\left(\theta_i + \varphi\right)}}, \tag{6b}$$

where $\theta_1 = 0$, $\theta_2 = \theta$, and φ is an integration variable. In this approximation, the integral over r can be carried out analytically, and the nonretarded Casimir-Lifshitz interaction energy per unit area is proportional to $1/d^2$.

The three dielectric constants in r_i^{pp} can be expressed in terms of two variables, such as $\varepsilon_\parallel/\varepsilon_3$ and $\varepsilon_\perp/\varepsilon_3$. Using Eqs. 5 and 6a, the integral over r in Eq. 2 can be performed analytically, and we can write the Hamaker coefficient as a sum of contributions from each Matsubara frequency:

$$A_\mathrm{Ham} = {\sum_{n=0}^{\infty}}' A_{\mathrm{Ham},n}, \tag{7a}$$

$$A_{\mathrm{Ham},n} = \frac{3k_\mathrm{B}T}{4\pi}\int_0^{2\pi} \mathrm{d}\varphi\ \mathrm{Li}_3\left(r_1^{pp} r_2^{pp}\right), \tag{7b}$$

where Li_3 is the third order polylogarithm function. The integration over φ is carried out numerically as a function of the ratios $\varepsilon_\parallel/\varepsilon_3$ and $\varepsilon_\perp/\varepsilon_3$ in Fig. 2.

The total Hamaker coefficient can be found by summing the values of the dielectric functions at each of the Matsubara frequencies. For comparison, we also consider the interaction between isotropic materials with $\varepsilon_1 = \varepsilon_\parallel$ and $\varepsilon_2 = \varepsilon_\perp$. The nonretarded free energy is given by Eq. 7, with $r_{i,\mathrm{iso}}^{pp} = \frac{\varepsilon_i - \varepsilon_3}{\varepsilon_i + \varepsilon_3}$. This expression yields Dzyaloshinskii's condition for repulsion between isotropic materials: $\varepsilon_1 < \varepsilon_3 < \varepsilon_2$ or $\varepsilon_2 < \varepsilon_3 < \varepsilon_1$. These conditions correspond to the blue region in Fig. 2(a).

By analogy, one might suspect that the repulsion condition for birefringent materials is $\varepsilon_\perp < \varepsilon_3 < \varepsilon_\parallel$ or, for materials with negative birefringence, $\varepsilon_\parallel < \varepsilon_3 < \varepsilon_\perp$. However, the repulsive condition depends on φ (the azimuthal direction of the mode's k-vector), and these inequalities are a necessary (but not sufficient) condition for repulsion. In the nonretarded case, the repulsion condition $r_1^{pp} r_2^{pp} < 0$, which yields a negative integrand in Eq. 7, simplifies to

$$\begin{aligned}&\left(\varepsilon_\perp\sqrt{1 + \left(\frac{\varepsilon_\parallel}{\varepsilon_\perp} - 1\right)\cos^2\varphi} - \varepsilon_3\right) \times \\ &\left(\varepsilon_\perp\sqrt{1 + \left(\frac{\varepsilon_\parallel}{\varepsilon_\perp} - 1\right)\cos^2\left(\theta + \varphi\right)} - \varepsilon_3\right) < 0.\end{aligned} \tag{8}$$

Systems that exhibit Casimir-Lifshitz repulsion (and, as a result, an attractive-repulsive transition with θ) will have materials that satisfy Eq. 8 for a range of φ at many Matsubara frequencies. In the anti-aligned case where $\theta = \pi/2$, this is achieved for combinations of dielectric functions that fall in the blue regions of Fig. 2(b). As an example of such a system, we consider a fictional material with high birefringence that has $\varepsilon_\parallel$ modeled by the dielectric response of gold and $\varepsilon_\parallel = 1$. We use the dispersion models from [14] and [29] for ethanol and gold, respectively. The points in Fig. 2b correspond to the $A_{\mathrm{Ham},n}$ that contribute to the repulsive nonretarded Casimir-Lifshitz force for this system. For comparison,

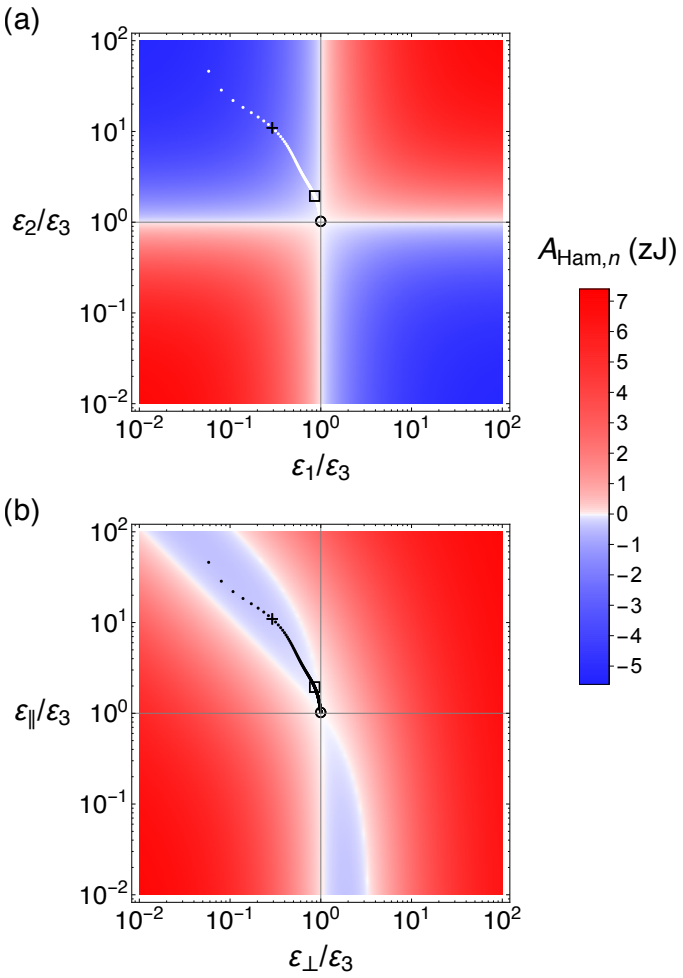

FIG. 2. The contribution of a single Matsubara term to the total Hamaker coefficient is plotted as a function of the dielectric coefficients. The red regions represent a positive energy (attractive force) and the blue regions represent a negative energy (repulsive force). (a) shows the contributions when the interacting materials are isotropic and not necessarily identical. (b) shows the contributions for two anti-aligned identical birefringent materials. The blue regions correspond to a negative contribution to the free energy (repulsion) for both (a) and (b). For anti-aligned birefringent materials, the greatest negative contribution possible from a single Matsubara term is approximately -0.45 zJ. The points indicate the contributions from the first 1000 Matsubara terms for the gold/ethanol/vacuum system (or gold gratings interacting across ethanol in (b)) at room temperature (Matsubara terms $n = 10, 100, 1000$ are indicated by $+, \square, \bigcirc$, respectively).

the points in Fig. 2a correspond to the nonretarded Casimir-Lifshitz interaction in a gold/ethanol/vacuum system.

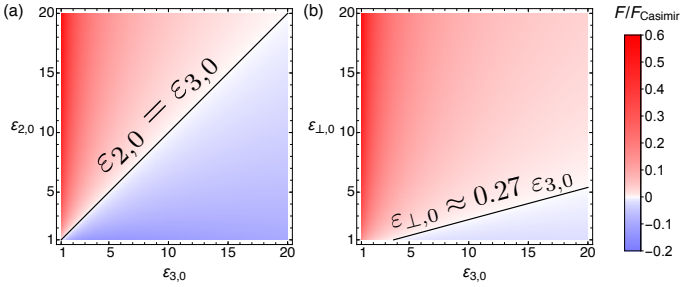

FIG. 3. The ratio of the zero-temperature, long-range Casimir force for two systems scaled to the Casimir force between two perfect conductors, ($F_{\mathrm{Casimir}} = -\hbar c\pi^2 240/d^4$), with $\varepsilon_{\parallel,0}$ and $\varepsilon_{1,0}$ taken to infinity (as for a perfect conductor). In this case, DC the dielectric constants of the other materials determine the sign of the force. For the isotropic case (a), the condition for repulsion is the usual $\varepsilon_{2,0} < \varepsilon_{3,0}$. For the case with identical, anti-aligned birefringent materials (b), the repulsive condition is numerically found to be $\varepsilon_{\perp,0} \lesssim 0.27\varepsilon_{3,0}$.

III. LONG-RANGE REPULSIVE CASIMIR FORCE BETWEEN ANISOTROPIC MATERIALS

At separations greater than a few nanometers, retardation effects become significant. The Hamaker coefficient usually decreases monotonically with distance, although it may be slightly increased in special cases [30]. The Casimir-Lifshitz force is a result of quantum fluctuations as well as thermal fluctuations, and the quantum fluctuations alone can cause repulsion between anti-aligned, birefringent materials. To illustrate this, we consider the long-range, zero-temperature Casimir effect. In this regime, the force between metals approaches the original expression derived by Casimir [1]: $F_{\mathrm{Casimir}}(d) = -\hbar c\ \frac{\pi^2}{240}\frac{1}{d^4}$. Lifshitz derived the force between dielectrics in the long-range case [2]. Physically, the DC dielectric constant $\varepsilon_{i,0}$ is used to describe the dielectric function over all frequencies because the high frequency terms are damped by retardation. With this approximation, we calculate the long-range Casimir force of anti-aligned gratings when the material is an ideal conductor ($\varepsilon \to \infty$) along its ordinary axes or extraordinary axis, which correspond to 2D and 1D conductors, respectively. When the material is a 1D conductor (Fig. 3), there is Casimir repulsion for anti-aligned materials when $\varepsilon_{\perp,0} \lesssim 0.27\varepsilon_{3,0}$. We note that long-range interactions at finite temperatures are dominated by the nonretarded $n = 0$ Matsubara term, which is strictly attractive for 1D conductors ($\varepsilon_\parallel \to \infty$). However, birefringent materials with finite dielectric functions at zero frequency may still exhibit long-range Casimir repulsion if the materials satisfy the conditions in Fig. 2(b) for the $n = 0$ term.

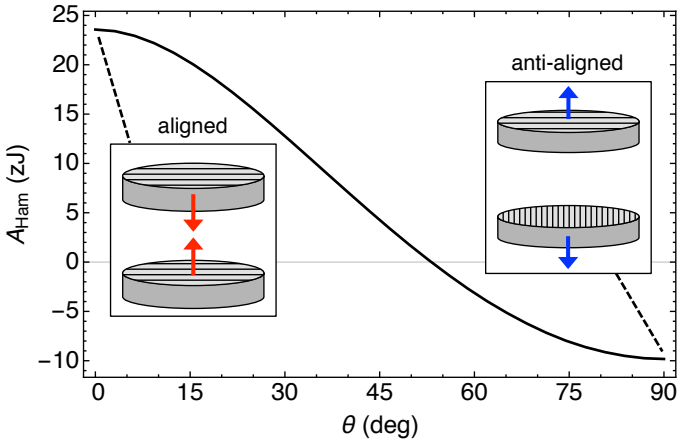

FIG. 4. The room temperature, nonretarded Hamaker constant between infinite half-spaces of 1D conductors ($\varepsilon_\perp = 1$, $\varepsilon_\parallel = \varepsilon_{\rm Au}$) separated by ethanol. The slabs experience an attractive force when the conduction axes are aligned, and a repulsive force when the axes are anti-aligned.

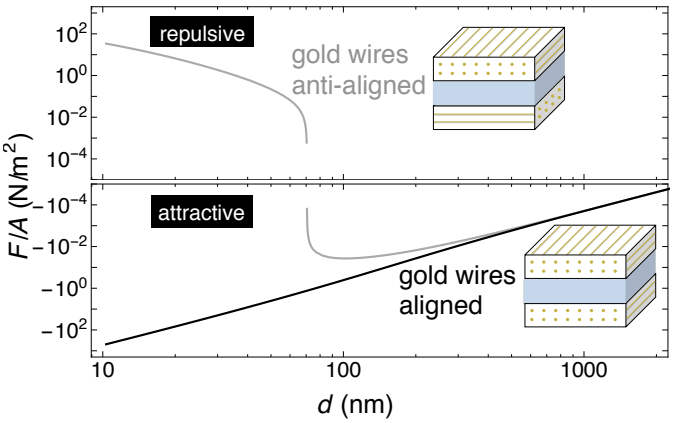

FIG. 5. The distance dependence of the Casimir-Lifshitz force between two idealized 1D conductors separated by ethanol. When the conductance directions are perpendicular, the two plates are repelled at short distances ($d \lesssim 70$ nm) and attracted at long distances.

IV. EXAMPLE WITH GOLD, ETHANOL, AND VACUUM

To illustrate some of the consequences of an orientation-dependent sign change in the Casimir force, we further consider the interaction between 1D gold conductors across ethanol with retardation effects: $\varepsilon_\parallel = \varepsilon_{\rm Au}$, $\varepsilon_\perp = 1$, $\varepsilon_3 = \varepsilon_{\rm ethanol}$ at room temperature. The anisotropic materials can be thought of as idealized arrays of gold nanowires. As noted in [31], the dielectric models used in calculation can have a nontrivial effect on the calculated results, so these calculations do not precisely represent the physical system. Instead, we present them to demonstrate the sign change in the Casimir force as a function of separation and relative orientation, and emphasize that this effect can occur for other combinations of materials.

At short ranges, this system exhibits attraction for aligned materials and repulsion for anti-aligned materials. The Hamaker coefficient is plotted as a function of relative orientation in Fig. 4. The extreme values of $A_{\rm Ham}$ correspond to $\approx 6\ k_{\rm B}T$ at room temperature, which is a typical value for dielectrics interacting across a medium [32]. We also show the energy of the aligned and anti-aligned materials as a function of distance in Fig. 5, noting that the energy has the approximate form of $\Omega(d,\theta) \sim \sin^2\theta$ at a fixed distance. The anti-aligned plates exhibit Casimir repulsion up to a separation of 70 nm. At greater distances the Casimir force is attractive. This sign change is a result of the dispersion of the materials, as in [33].

V. CASIMIR-LIFSHITZ REPULSION BETWEEN REAL MATERIALS

We have calculated the repulsive force between the hypothetical gold/vacuum gratings in ethanol to demonstrate a strong version of this effect. However, the gratings would surely have different dielectric properties than the simple $\varepsilon_\perp = 1$, $\varepsilon_\parallel = \varepsilon_{\rm Au}$ system we have described here. In reality, one might consider the effect between two identical, uniaxial crystals with high optical anisotropy. The calculation of Casimir-Lifshitz forces requires the knowledge of $\varepsilon(i\xi)$ for a very large range of frequencies. These dielectric functions can be constructed from optical data with the Kramers-Kronig relations but usually carry a large degree of uncertainty [32, 34–36]. The repulsive force discussed here requires an intervening dielectric of intermediate strength at a large number of Matsubara terms so given the limited availability of experimentally determined optical properties, it is difficult to confidently predict a combination of materials that could achieve repulsion.

However, we can suggest properties of materials that could achieve a repulsive force. With an eye towards satisfying Eq. 8, we suggest that the uniaxial crystals should have high birefringence. If the intervening material is a liquid, then uniaxial crystals with low indices may make the repulsion condition easier to satisfy (as many liquids have $1 < \varepsilon(i\xi) < 2$ for the relevant Matsubara frequencies [36]). A system that satisfies Eq. 8 for the $n = 0$ Matsubara term, for which static dielectric constants are often well-known, would likely achieve repulsion at large separations where the $n = 0$ term dominates.

In Fig. 6, we plot dielectric models of $\varepsilon(i\xi)$ for four birefringent materials along with $\varepsilon(i\xi)$ models for liquids that satisfy Eq. 8 for some Matsubara terms. We construct Ninham-Parsegian models for $\varepsilon(i\xi)$ of BaB_2O_4

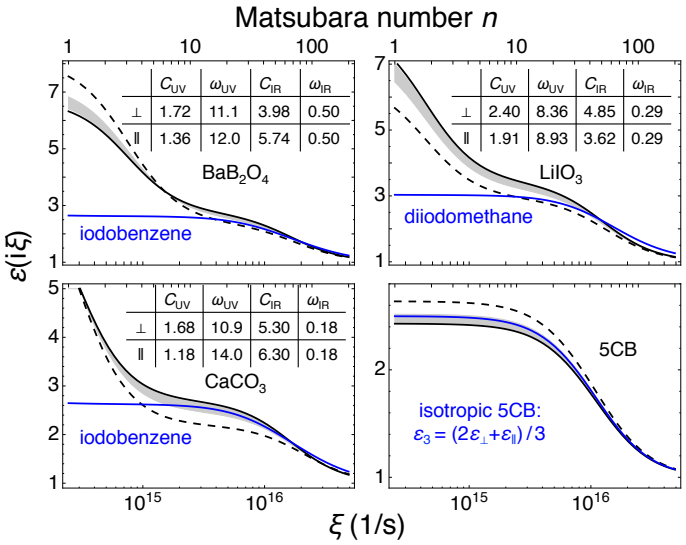

FIG. 6. The black lines represent the birefringent crystals with solid and dashed lines corresponding to the ordinary ($\perp$) and extraordinary ($\parallel$) axes, respectively. The gray band represents values of $\varepsilon_3(i\xi)$ that satisfy Eq. 8. The blue lines represent a liquid chosen to maximize the number of Matsubara terms that satisfy Eq. 8. Inset are the values used in the Ninham-Parsegian oscillator model, with values for $\omega_{\rm UV}$ and $\omega_{\rm IR}$ in eV.

and $LiIO_3$ using the method of [34], the static dielectric constants from [37], and the optical data from [38] and [39]. The model for $CaCO_3$ is from [35], and the models for iodobenzene and diiodomethane are from [36]. With these dielectric models, the systems with BaB_2O_4, $LiIO_3$, and $CaCO_3$ and chosen liquids would not experience Casimir-Lifshitz repulsion for any relative orientation of the crystals. However, given our limited knowledge of the $\varepsilon(i\xi)$ functions, it is possible that the proposed systems or others like them could exhibit the repulsive effect described here for slightly modified optical properties.

A system that often satisfies Eq. 8 is the intervening 'melt' between two birefringent solids considered by Parsegian [5], which has $\varepsilon_3 = (2\varepsilon_\perp + \varepsilon_\parallel)/3$. This is a common model for liquid crystals in the isotropic state [41]. The lower right figure in Fig. 6 shows the interaction between anti-aligned 5CB nematic liquid crystal when separated by isotropic 5CB. This uses the dispersion model for 5CB developed in [40]. However, measuring a repulsive force between two liquid layers (separated by a third liquid at a different temperature) presents obvious experimental difficulties.

VI. CONCLUSION

We have detailed the conditions for a repulsive Casimir-Lifshitz force to exist between identical birefringent materials in the retarded and nonretarded regimes. The constraint on the dielectric functions (Eq. 8) is more restrictive than the $\varepsilon_1 < \varepsilon_3 < \varepsilon_2$ condition for isotropic dielectrics. However, repulsion between identical birefringent materials is achievable. Furthermore, because the force can be changed from attractive to repulsive by rotating one of the materials, it could be used as a switchable force in MEMS or NEMS devices. Because repulsion between identical birefringent dielectrics exists for certain materials over a large range of separations, this effect could be important in many physical systems.

Appendix: Compact notation for dispersion relation

The explicit form of the dispersion relation ($D_n = 0$) for two uniaxial, anisotropic, parallel plates with optical axes in-plane is written [4, 14, 27]. The full form is cumbersome and opaque [30], but can be written much more compactly in terms of the Fresnel reflection matrix for each plate:

$$D_n = \det\left(\mathbf{1} - \boldsymbol{r}_1\boldsymbol{r}_2 e^{-2\rho_3 d}\right). \tag{A.1}$$

For each plate, the Fresnel reflection coefficients can be written in terms of a common denominator:

$$\boldsymbol{r} = \begin{pmatrix} r_{ss,\mathrm{N}} & r_{sp,\mathrm{N}} \\ r_{ps,\mathrm{N}} & r_{pp,\mathrm{N}} \end{pmatrix} / r_{\mathrm{D}}. \tag{A.2}$$

$$r_{sp,\mathrm{N}} = r_{ps,\mathrm{N}} = k\sqrt{\varepsilon_3}\varepsilon_\perp \rho_i \rho_3 \left(\rho_i - \widetilde{\rho}_i\right) \sin\left(2\theta_i\right) \tag{A.3a}$$

$$r_{ss,\mathrm{N}} = \sin^2\left(\theta_i\right) \widetilde{\alpha_-}\gamma_+ + \cos^2\left(\theta_i\right) \alpha_- \nu_+ \tag{A.3b}$$

$$r_{pp,\mathrm{N}} = -\sin^2\left(\theta_i\right) \widetilde{\alpha_+}\gamma_- + \cos^2\left(\theta_i\right) \alpha_+ \nu_- \tag{A.3c}$$

$$r_{\mathrm{D}} = \sin^2\left(\theta_i\right) \widetilde{\alpha_+}\gamma_+ + \cos^2\left(\theta_i\right) \alpha_+ \nu_+ \tag{A.3d}$$

Where we have introducted the following notation, which is modeled after [42, 43]:

$$\alpha_\pm = \rho_3 \pm \rho_i \tag{A.4a}$$

$$\widetilde{\alpha_\pm} = \rho_3 \pm \widetilde{\rho}_i \tag{A.4b}$$

$$\nu_\pm = \varepsilon_3 \rho_i^3 \pm \varepsilon_\perp \rho_i \widetilde{\rho}_i \rho_3 \tag{A.4c}$$

$$\gamma_\pm = \varepsilon_\perp k^2 \left(\varepsilon_\perp \rho_3 \pm \varepsilon_3 \rho_i\right). \tag{A.4d}$$

This uses the original notation of Barash:

$$\rho_i = \sqrt{r^2 + \varepsilon_\perp k^2} \tag{A.5a}$$

$$\rho_3 = \sqrt{r^2 + \varepsilon_3 k^2} \tag{A.5b}$$

$$\widetilde{\rho}_i = \sqrt{r^2 + \left(\varepsilon_\parallel/\varepsilon_\perp - 1\right) r^2 \cos^2\theta_i + \varepsilon_\parallel k^2} \tag{A.5c}$$

with $k = \xi/c$ (where ξ is an imaginary frequency) and θ_i representing the azimuthal angle between the wavevector and extraordinary axis of the material. If we choose coordinates such that the extraordinary axis of the first birefringent plate is along the x-axis, then $\theta_1 = \varphi$ and $\theta_2 = \varphi + \theta$, where φ is an integration variable and

θ is the relative angle between the two crystals' extraordinary axes. With these substitutions, this formulation reproduces the analytic formula of [4]. We hope that this notation can help to elucidate these complicated interactions.

[1] H. Casimir, Proc. K. Ned. Akad. Wet **51** (1948).
[2] E. Lifshitz, J. Exper. Theor. Phys. **2**, 73 (1956).
[3] I. E. Dzyaloshinskii, E. M. Lifshitz, and L. P. Pitaevskii, Sov. Phys. Uspekhi **4**, 153 (1961).
[4] Y. S. Barash, Izv. Vyss. Uchebnykh Zaved. Radiofiz. **21**, 1637 (1978).
[5] V. A. Parsegian and G. H. Weiss, J. Adhes. **3**, 259 (1972).
[6] S. K. Lamoreaux, Phys. Rev. Lett. **78**, 5 (1997).
[7] J. N. Munday, F. Capasso, and V. A. Parsegian, Nature **457**, 170 (2009).
[8] R. Decca, D. López, E. Fischbach, G. Klimchitskaya, D. Krause, and V. Mostepanenko, Ann. Phys. (N. Y). **318**, 37 (2005).
[9] H. B. Chan, Science (80-.). **291**, 1941 (2001).
[10] G. Bressi, G. Carugno, R. Onofrio, and G. Ruoso, Phys. Rev. Lett. **88**, 041804 (2002).
[11] U. Mohideen and A. Roy, Phys. Rev. Lett. **81**, 4549 (1998).
[12] X. Chen and J. C. H. Spence, Phys. status solidi **248**, 2064 (2011).
[13] O. Kenneth and S. Nussinov, Phys. Rev. D **63**, 121701 (2001).
[14] J. N. Munday, D. Iannuzzi, Y. Barash, and F. Capasso, Phys. Rev. A **71**, 042102 (2005).
[15] J. N. Munday, D. Iannuzzi, and F. Capasso, New J. Phys. **8**, 244 (2006).
[16] D. A. T. Somers and J. N. Munday, Phys. Rev. A **91**, 032520 (2015).
[17] F. M. Serry, D. Walliser, and G. J. Maclay, J. Appl. Phys. **84**, 2501 (1998).
[18] M. Ishikawa, N. Inui, M. Ichikawa, and K. Miura, J. Phys. Soc. Japan **80**, 114601 (2011).
[19] T. H. Boyer, Phys. Rev. A **9**, 2078 (1974).
[20] O. Kenneth, I. Klich, A. Mann, and M. Revzen, Phys. Rev. Lett. **89**, 033001 (2002).
[21] V. K. Pappakrishnan, P. C. Mundru, and D. A. Genov, Phys. Rev. B **89**, 045430 (2014).
[22] F. S. S. Rosa, D. A. R. Dalvit, and P. W. Milonni, Phys. Rev. A **78**, 032117 (2008).
[23] M. Levin, A. P. McCauley, A. W. Rodriguez, M. T. H. Reid, and S. G. Johnson, Phys. Rev. Lett. **105**, 090403 (2010).
[24] M. F. Maghrebi, Phys. Rev. D **83**, 045004 (2011).
[25] G. Deng, Z.-Z. Liu, and J. Luo, Phys. Rev. A **78**, 062111 (2008).
[26] O. Kenneth and I. Klich, Phys. Rev. Lett. **97**, 160401 (2006).
[27] J. N. Munday, D. Iannuzzi, Y. Barash, and F. Capasso, Phys. Rev. A **78**, 029906(E) (2008).
[28] A. Lambrecht, P. A. M. Neto, and S. Reynaud, New J. Phys. **8**, 243 (2006).
[29] R. Decca, D. López, E. Fischbach, G. Klimchitskaya, D. Krause, and V. Mostepanenko, Eur. Phys. J. C **51**, 963 (2007).
[30] D. M. Dryden, J. C. Hopkins, L. K. Denoyer, L. Poudel, N. F. Steinmetz, W.-Y. Ching, R. Podgornik, A. Parsegian, and R. H. French, Langmuir **31**, 10145 (2015).
[31] P. J. Van Zwol and G. Palasantzas, Phys. Rev. A **81**, 062502 (2010).
[32] V. A. Parsegian, *Van der Waals Forces* (Cambridge University Press, Cambridge, 2005).
[33] M. Boström, B. E. Sernelius, I. Brevik, and B. W. Ninham, Phys. Rev. A **85**, 010701 (2012).
[34] D. B. Hough and L. R. White, Adv. Colloid Interface Sci. **14**, 3 (1980).
[35] L. Bergström, Adv. Colloid Interface Sci. **70**, 125 (1997).
[36] P. J. van Zwol, G. Palasantzas, and J. T. M. De Hosson, Phys. Rev. B **79**, 195428 (2009).
[37] G. G. Gurzadyan and P. Tzankov (Springer Berlin Heidelberg, 2005) pp. 817–901.
[38] M. M. Choy and R. L. Byer, Phys. Rev. B **14**, 1693 (1976).
[39] D. Eimerl, L. Davis, S. Velsko, E. K. Graham, and A. Zalkin, J. Appl. Phys. **62**, 1968 (1987).
[40] P. E. Kornilovitch, J. Phys. Condens. Matter **25**, 035102 (2013).
[41] W. Maier and G. Meier, Zeitschrift für Naturforsch. A **16**, 262 (1961).
[42] J. Lekner, J. Phys. Condens. Matter **3**, 6121 (1991).
[43] J. Lekner, J. Opt. Soc. Am. A **10**, 2059 (1993).